

用于去除有机染料的分级结构 ZnO 微球的简便合成

孙同明 尤 梦 王丹琪 崔 莹 崔会会 王 森* 汤艳峰*

(南通大学化学化工学院, 南通 226019)

摘要: 以六亚甲基四胺(HMTA)为结构导向剂,采用乙二醇辅助的溶剂热法制备了均匀分散的纳米片组装的三维分级结构 ZnO 微米球。可控实验证明,HMTA 和溶剂在分级结构微米球的形成中起重要作用。通过二维纳米片组装来构建三维分级结构,不仅增加了产品的比表面积,而且还建立了更多的电荷传输通道。在暗室下,该样品可作为吸附剂去除水溶液中的一些有机染料。吸附结果表明,纳米片组装的分级结构 ZnO 微球对阴离子染料具有良好的去除率和选择性。特殊的分级结构、较大的比表面积和静电引力的协同作用,使 ZnO 微球对代表性染料刚果红(CR)经过5次循环吸附后的去除率仍可达95.67%。动力学研究证实,CR在 ZnO 微球上的吸附为物理吸附,符合准二级动力学和 Langmuir 等温线模型。

关键词: ZnO; 分级结构; 纳米材料; 有机染料; 吸附

中图分类号: O614.24¹ 文献标识码: A 文章编号: 1001-4861(2023)06-1131-08

DOI: 10.11862/CJIC.2023.067

Simple synthesis of hierarchical ZnO microspheres for organic dyes removal

SUN Tong-Ming YOU Meng WANG Dan-Qi CUI Ying

CUI Hui-Hui WANG Miao* TANG Yan-Feng*

(School of Chemistry and Chemical Engineering, Nantong University, Nantong, Jiangsu 226019, China)

Abstract: Uniform and dispersed 3D hierarchical nanosheets-assembled ZnO microspheres were fabricated by a simple ethylene glycol (EG)-assisted solvothermal route, in which hexamethylenetetramine (HMTA) was selected as a functional agent. A series of controllable experiments proved that HMTA and the solvent play vital roles in the formation of hierarchical microspheres. The assembly of 2D nanosheets to construct the 3D hierarchical structures not only increases the specific surface area of the products but also builds more charge transport channels. The samples were evaluated as adsorbents for the removal of some organic dyes from the aqueous solution in dark. Resultantly, the hierarchical nanosheets-assembled ZnO microspheres showed excellent removal rate and selectivity for anionic dyes. Taking Congo red (CR) as a representative dye, it can be removed 95.67% after five adsorption cycles due to the synergistic effects of hierarchical structures, large surface areas, and electrostatic attraction. The kinetics studies confirmed that the adsorption of CR onto ZnO microspheres is physisorption and followed the pseudo-second-order kinetic and Langmuir isotherm models.

Keywords: ZnO; hierarchical structures; nanomaterials; organic dyes; adsorption

Nowadays, water is under constant threat from various organic pollutants, which seriously affect human production and life. As one of the wastewater

treatment technology, the adsorption method has been widely utilized for its numerous advantages, such as easy operation, great selectivity, and no pollution^[1-5].

收稿日期:2023-03-02。收修改稿日期:2023-04-14。

国家自然科学基金(No.22075152)、江苏省大学生创新训练项目(No.202210304023Z, 202210304099Y)和南通大学大型仪器开放测试基金(No.KFJN2206, KFJN2211, KFJN2214)资助。

*通信联系人。E-mail: wangmiao@ntu.edu.cn, tangyf@ntu.edu.cn

However, the relatively high price and low treatment efficiency of many conventional adsorbents limit their practical large-scale application. Therefore, exploring low-cost and eco-friendly adsorbents with high efficiency is desirable for the elimination of toxic chemicals from the environment. In the past decades, various semiconductor catalysts have been explored as prospective adsorbents to remove organic contaminants from wastewater. Among the semiconductor materials, ZnO has attracted extensive attention due to its unique properties originating from its suitable band structure, high stability, low cost, nontoxic and tuneable morphologies^[6-10]. However, compared with a large amount of research on photocatalytic properties, less attention has been paid to the studies of ZnO as an adsorbent in wastewater treatment^[14-15].

It has been reported that optimized geometric configuration and structure are key roles in improving adsorption performances. From this view, with a large surface area and porous structures, micro/nanoscaled 3D hierarchical architectures might provide more open pore channels and more active sites to accelerate the electron transfer rate, thereby leading to substantial improvement of their adsorption efficiency. So far, a large number of adsorbents with 3D hierarchical nano/microstructures have been fabricated^[16-20]. Given the advantages of ZnO, therefore, it is urgent to develop novel 3D hierarchical ZnO adsorbents for further effectively improving the adsorption performances and extending their potential applications in wastewater treatment.

Enlightened by the above hierarchical architectures, herein, a simple solvothermal route was explored to prepare 3D hierarchical ZnO microspheres, in which hexamethylenetetramine (HMTA) and the solvent ratio play vital roles in the formation of different morphological ZnO nano/microstructures. Furthermore, the adsorption activities of as-obtained ZnO were investigated by the degradation of various organic dyes of aqueous solution in dark. The equilibrium kinetics studies indicate that the adsorption is a physisorption process and follows the Langmuir isotherm and pseudo-second-order model.

1 Experimental

1.1 Materials

All the reagents were analytical grade and used without further purification. Ethylene glycol (EG), HMTA, and $\text{Zn}(\text{OAc})_2 \cdot 2\text{H}_2\text{O}$ were supplied by Shanghai Macklin Biochemical Co., Ltd. Congo red (CR), and other organic dyes such as new carmine (NC), methyl orange (MO), methyl violet (MV), methylene blue (MB), and rhodamine B (RhB) were provided by Shanghai Sinopharm Group Chemical Reagent Co., Ltd.

1.2 Characterization

The crystalline phases of the products were analyzed by XRD on a Bruker D8-Advance powder X-ray diffractometer (Cu $K\alpha$ radiation, $\lambda = 0.15418$ nm), employing a scanning rate of 4.00 ($^\circ$) $\cdot \text{min}^{-1}$ in a 2θ range from 10° to 80° . The operation voltage and current were maintained at 40 kV and 40 mA, respectively. The sizes and morphologies of the resulting products were studied by field emission scanning electron microscopy (FE-SEM, Zeiss Gemini 300) at 15 kV. Fourier transforms infrared (FTIR) spectra and ultraviolet-visible (UV-Vis) absorption spectra were collected using the Nicolet Avatar 370 FT-IR spectrophotometer and Shimadzu UV-3600 spectrophotometer respectively. N_2 adsorption-desorption on Micromeritics ASAP 2020C apparatus was employed to further investigate the porous structure of as-prepared adsorbents. The ζ potential of the product was measured by Malvern Zetasizer Nano ZS90.

1.3 Synthesis of nanosheets-assembled hierarchical ZnO microspheres

In a typical process, 1 mmol $\text{Zn}(\text{OAc})_2 \cdot 2\text{H}_2\text{O}$ and 1 mmol HMTA were homogeneously diffused in 25 mL EG by magnetic stirring for 30 min. Then the mixture solution was poured into a 30 mL Teflon-lined stainless-steel autoclave and kept at 120 $^\circ\text{C}$ for 12 h. After cooling to room temperature, the white precipitate was collected by centrifugation, washed with ethanol aqueous several times, and dried at 70 $^\circ\text{C}$ for 3 h. For comparison, different morphological ZnO was also prepared according to a similar process except for the different amounts of HMTA (0, 0.5 mmol) and different volume

ratios of EG/H₂O ($V_{EG} : V_{H_2O} = 0:25, 5:20, 12.5:12.5, 20:5$).

1.4 Adsorption experiments

Typically, 20.0 mg of ZnO powders were dispersed into 40 mL 20 mg·L⁻¹ of CR aqueous solution under magnetic stirring (1 000 r·min⁻¹) at room temperature. During the adsorption, 3.5 mL of suspension was sampled from the reactor at a fixed time interval and centrifuged to remove the residual powders. After adsorption, the supernatant and precipitated powders were collected individually. To study the adsorption selectivity of ZnO, several other organic dyes were chosen as simulated pollutants including NC, MO, MB, MV, and RhB. The effect of CR solution concentrations (20 - 150 mg·L⁻¹) on the adsorption process was also studied in detail. The molecular structure of CR is shown in Fig.1.

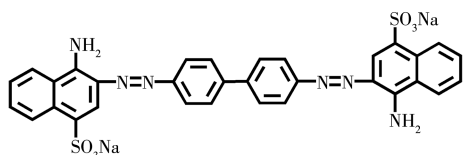


Fig.1 Molecular structure of CR

2 Results and discussion

The XRD pattern of the product obtained in the typical procedure is shown in Fig.2a. Clearly, all dif-

fraction peaks are in good agreement with the hexagonal phase of ZnO (PDF No.36-1451). N₂ adsorption-desorption isotherms were measured to determine the surface area of as-obtained ZnO, and the corresponding results are presented in Fig.2b. The isotherm displayed a typical IV isotherm of a type H3 hysteresis loop at a relative pressure (p/p_0) between 0.6 and 1.0, strongly indicating the presence of mesopores in the products. The Brunauer-Emmett-Teller (BET) surface of the hierarchical ZnO microspheres was 106 m²·g⁻¹. A high specific surface area is beneficial to provide more active sites and improve the adsorptive performance. The morphology and microstructural characterizations of ZnO were investigated by SEM. As displayed in Fig. 2c, there are numerous uniform microspheres with a diameter of 1-1.5 μm. The magnified SEM image from a single microsphere (Fig.2d) reveals that there are covering many curved nanosheets on an irregular surface. Further enlarged the SEM image, some distinct lamellar structures were observed, and the thickness of the nanosheet was about 20 nm (Fig. 2e). These unique structures might provide sufficient pores, larger specific surface, more transportation channels, and better contact of organic pollutants, benefiting its adsorption performance.

To reveal the role of HMTA and the possible mechanism, a series of control experiments were sys-

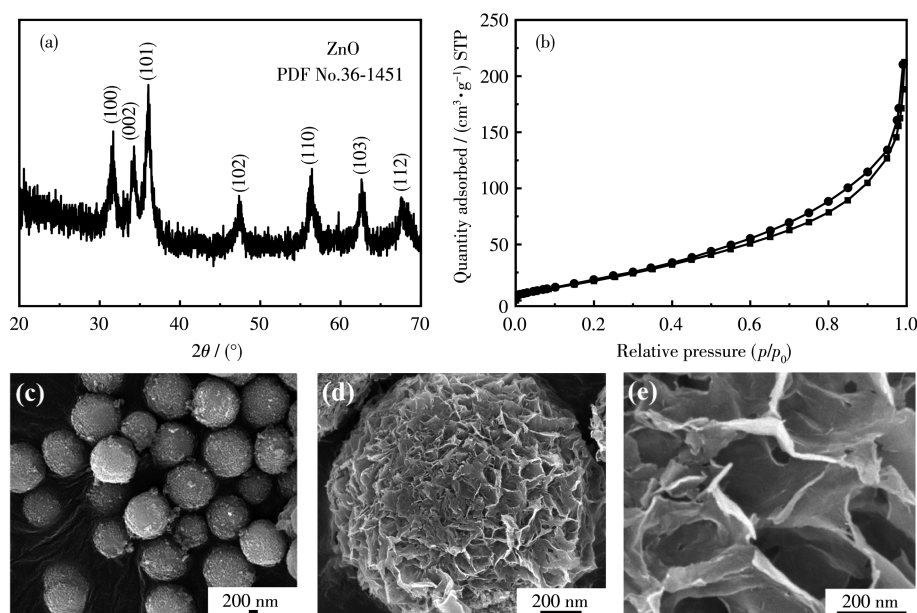


Fig.2 XRD pattern (a), N₂ adsorption-desorption isotherm (b), and SEM images (c-e) of the typical ZnO

tematically conducted by adjusting the amounts of HMTA (0, 0.5, 1 mmol), and the morphologies of the products are listed in SEM image (Fig. 3a - 3c). As shown in Fig. 3a, nanoparticle-assembled microspheres with a diameter of approximately 1.5 μm were obtained without HMTA. After 0.5 mmol HMTA was added, the microspheres were composed of nanoparticles and nanosheets (Fig. 3b). When the amount of HMTA exceeded 1 mmol, the morphologies of nanosheets - assembled microspheres were maintained (Fig. 3c). Therefore, as the amount of HMTA increases, the product tends to form nanosheets-assembled microspheres. Previous work has proved that HMTA molecules can adjust and modify the morphology of micro/nanostructures by preferentially interacting with certain crystal faces^[21-26]. Herein, HMTA not only provides an alkaline environment but also acts as the functional agent coordinating with Zn^{2+} for subsequent crystal growth. Therefore, HMTA is crucial in the controllable fabrication of hierarchical nanosheets-assembled microspheres.

To investigate the effects of the EG on the morphology of the products, a series of contrast experiments were performed by varying EG volumes (20, 12.5, 5, and 0 mL) when 1 mmol of HMTA was used.

The corresponding SEM images are shown in Fig. 3d-3g. Nanosheets - assembled irregular aggregates were formed in the presence of 20 mL EG (Fig. 3d). Decreasing the EG volume to 12.5 mL, the mixture of nanosheets and nanorods was prepared, as shown in Fig. 3e. Further lowering the EG volume to 5 and 0 mL, nanorod-assembled dumbbell and nanorods (Fig. 3f-3g) were obtained, respectively. From the morphological evolution, without EG, or when the volume of EG was less than 12.5 mL, the main morphology of the products was 1D nanorods. Enough EG molecule is favorable to the nanosheet assembled process and thereby the formation of spherical structures, which are consistent with the previous work^[27-30]. As a polyol, the hydroxyl groups in EG molecules will coordinate with metal ions to further control the crystallization process and subsequent growth direction. Therefore, acting as a solvent and structure-directing agent, the EG molecule is a key role in the formation of ZnO with different shapes. The growth rates of ZnO nuclei along different crystal directions could be precisely controlled by changing the ratio of EG/ H_2O . Fig.S1 (Supporting information) shows the XRD patterns of as-prepared ZnO samples with different amounts of HMTA and different

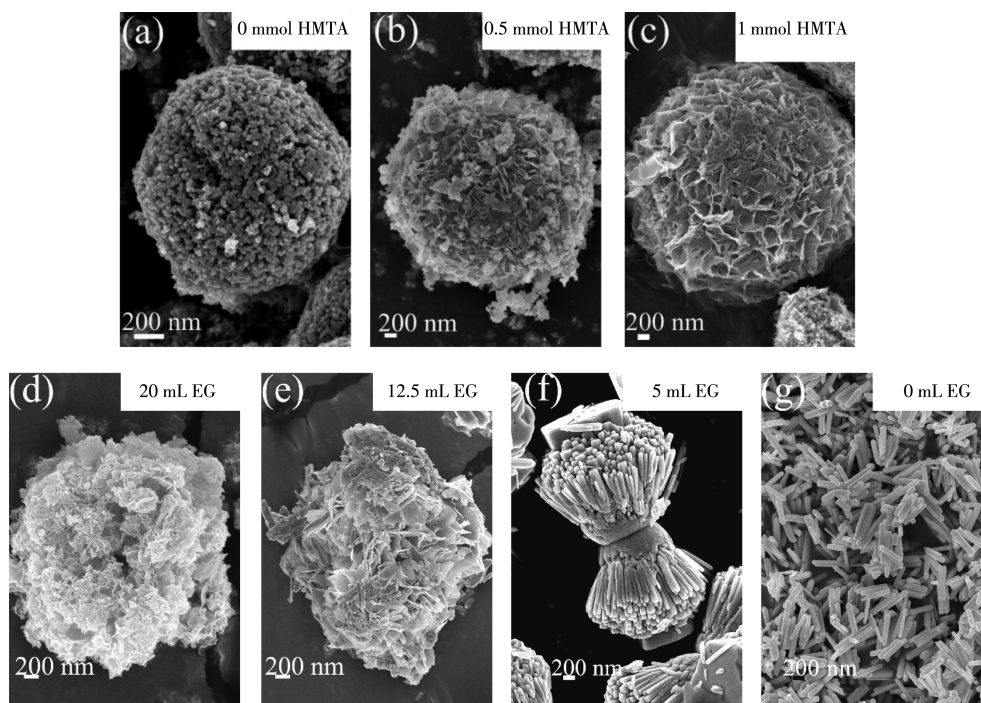


Fig.3 SEM images of ZnO obtained from different amounts of HMTA: (a) 0 mmol; (b) 0.5 mmol; (c) 1 mmol; SEM images of ZnO obtained from different volumes of EG: (d) 20 mL; (e) 12.5 mL; (f) 5 mL; (g) 0 mL

volumes of EG. All products were indexed to the pure hexagonal phase of ZnO.

Different kinds of organic dyes ($20 \text{ mg} \cdot \text{L}^{-1}$), such as anionic dyes (CR, MO, NC) and cationic dyes (RhB, MV, MB) were selected as simulate pollutants to investigate the adsorption performance of hierarchical ZnO microspheres. The color photographs before and after adsorption and removal rate of dyes within 60 min are shown in Fig. 4a and 4b. Taking the CR dyes as an example, the degradation rate was up to 100%. The nanosheets-assembled hierarchical ZnO microspheres exhibited excellent adsorption selectivity to anionic dyes. As shown in Fig. 1, CR is an anionic dye with a

complex aromatic structure, which provides it stability against oxidizing agents and thus makes it non-biodegradable. Other anionic dyes, such as MO and NC also have been removed efficiently by the hierarchical ZnO microspheres. On the contrary, compared with anionic dyes, the removal rate of cationic dyes (RhB, MV, MB) decreased significantly. The charge of the ZnO powders was investigated and the ζ potential was $+23.2 \text{ mV}$ in water (Inset of Fig. 4b). Therefore, owing to the electrostatic attraction between positive charged hierarchical ZnO microspheres and anionic organic dyes, hierarchical ZnO microspheres feature outstanding adsorption selectivity. The adsorption performance

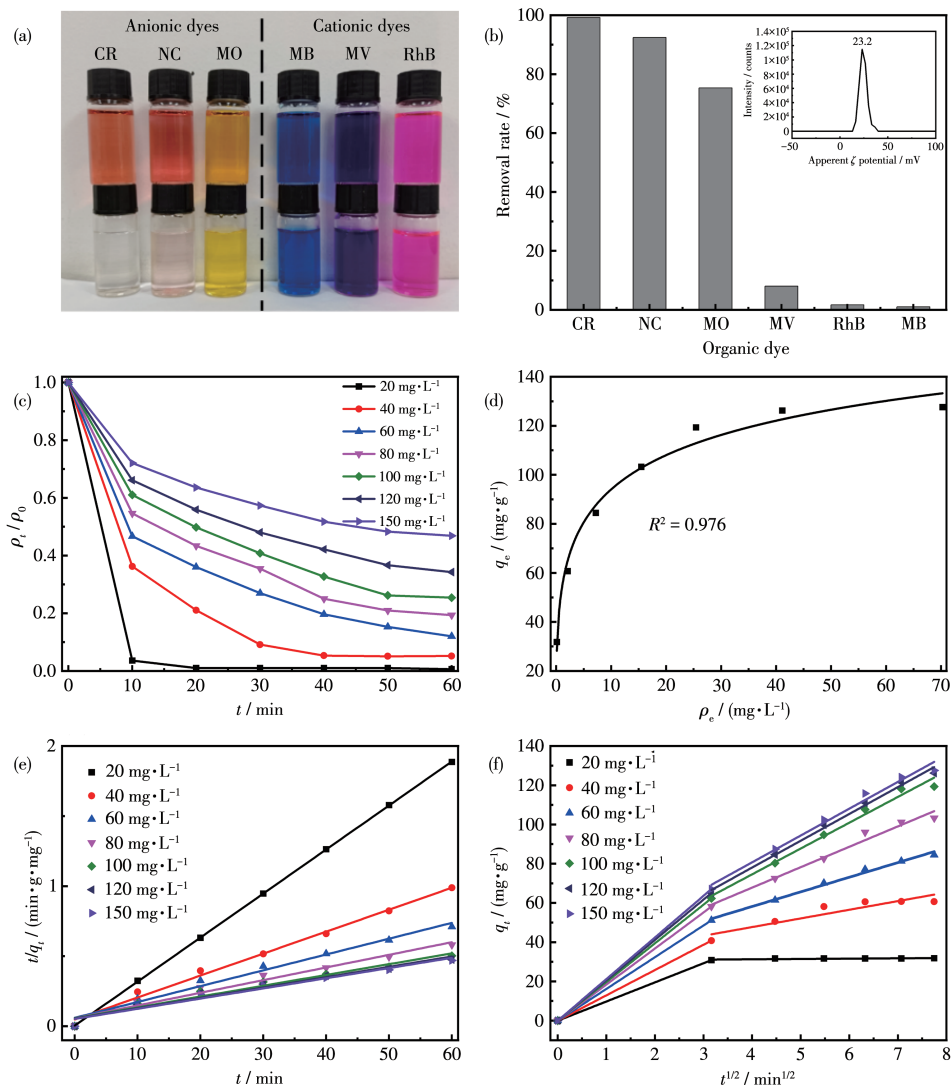


Fig. 4 (a) Photographs before and after adsorption, and (b) removal rates ($20 \text{ mg} \cdot \text{L}^{-1}$) of different dyes and ζ potential of typical ZnO (Inset); (c) Adsorption efficiency, (d) Langmuir adsorption isotherm, (e) pseudo-second-order kinetic curves, and (f) intra-particle diffusion model curves with different concentration of CR ($20\text{-}150 \text{ mg} \cdot \text{L}^{-1}$)

of the ZnO microspheres towards different concentrations of CR ($20\text{--}150\text{ mg}\cdot\text{L}^{-1}$) was also investigated. As shown in Fig. 4c, in the presence of adsorbents, 100% of CR ($20\text{ mg}\cdot\text{L}^{-1}$) was degraded in 10 min. The removal rate was about 50% in 60 min when the concentration of CR dye solution was increased several times up to $150\text{ mg}\cdot\text{L}^{-1}$, suggesting the ZnO microspheres exhibited great efficiency. Obviously, with the increase of the CR concentration, the adsorption dosage increased greatly until it reached saturation. After a batch of data analysis, the adsorption performances of hierarchical ZnO microspheres were well fitted with the Langmuir adsorption isotherm (Fig. 4d) and the pseudo-second-order kinetic curve (Fig. 4e) with correlation coefficients as 0.976 and 0.999, respectively. The maximum adsorption capacity (q_m) of CR was $221.82\text{ mg}\cdot\text{g}^{-1}$ from the Langmuir isotherm model. Furthermore, the adsorption kinetics of hierarchical ZnO microspheres was investigated. As shown in Fig. 4f, for each concentration of CR aqueous solution, there were two different parts of plots were observed at the early and late periods during the adsorption process, revealing that the adsorption rates were changed. In general, the larger the slope, the faster the adsorption. The steeper line at the beginning is ascribed to the diffusion of CR molecules from the aqueous solution to the surface of adsorbents. The subsequent smooth and slow line is an index to the intra-particle diffusion. In this work, it is obvious that the intra-particle diffusion stage is the most important dominant step in determining the

adsorption rate.

As well known, morphology is a key factor in the adsorption process. Therefore, the effects of different morphological micro/nanostructures on the adsorption performances were tested by the degradation of $20\text{ mg}\cdot\text{L}^{-1}$ CR aqueous solution. As shown in Fig. S2, the removal rate of nanosheets-assembled microspheres of ZnO was much higher than that of other morphological ZnO nano/microstructures, implying these unique microspheres were of excellent adsorption performances. It is ascribed to the synergistic effects of larger BET surface area and novel hierarchical structures.

To ascertain the nature of the adsorption process, the FTIR spectra and XRD patterns of the typical ZnO before and after adsorption were investigated and the results are provided in Fig. 5a and 5b. The peaks of CR were observed in FTIR results of post-adsorption ZnO samples, which are attributed to the strong electrostatic interaction and outstanding adsorption properties. No diffraction peaks of other chemicals were observed in XRD patterns except ZnO. These FTIR and XRD observations confirm that the adsorption is not chemical but a physisorption process. The cyclical stability of adsorbents is of great importance for long-term use in practice. Fig. 5c shows the cycle adsorption performances of hierarchical ZnO microspheres in dark. The removal rate remained at 95.67% after 5 cycles, indicating that the hierarchical ZnO microspheres are of good chemical stability and can be employed as adsorbents in practical applications.

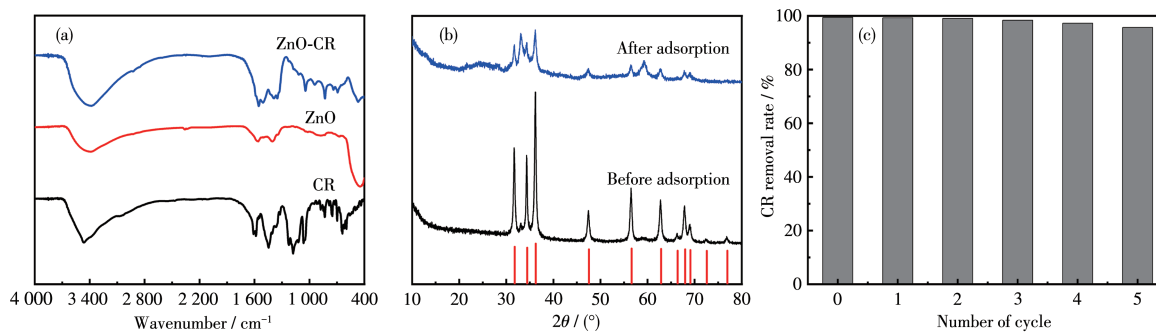


Fig. 5 FTIR spectra (a) and XRD patterns (b) of the ZnO before and after adsorption; (c) Cyclic adsorption performance

3 Conclusions

A simple EG-assisted solvothermal method

was developed for the synthesis of nanosheet-assembled hierarchical ZnO microspheres. The amount of HMTA and the ratio of EG/H₂O play cru-

cial roles in the formation of different morphological ZnO micro/nanostructures. Nanosheets-assembled hierarchical ZnO microspheres exhibited outstanding efficiency and selectivity toward anionic CR dye. Up to 100% removal rate was achieved in 10 min, and a 95.67% removal rate after five adsorption cycles, which will enable it to have a wide application in adsorption fields. The excellent performance is ascribed to the synergistic effects of the hierarchical porous structures and the larger specific areas during the adsorption process. Our work may provide a rational design strategy to prepare other hierarchical architectures and as-obtained hierarchical ZnO microspheres can be applied as eco-friendly, efficient, and reusable adsorbents for wastewater treatment.

Supporting information is available at <http://www.wjhxxb.cn>

References:

- [1]Kausar A, Iqbal M, Javed A, Aftab K, Nazli Z H, Bhatti H N, Nouren S. Dyes adsorption using clay and modified clay: A review. *J. Mol. Liq.*, **2018**,**256**:395-407
- [2]Molla A, Li Y, Mandal B, Kang S G, Hur S H, Chung J S. Selective adsorption of organic dyes on graphene oxide: Theoretical and experimental analysis. *Appl. Surf. Sci.*, **2019**,**464**:170-177
- [3]Yu F, Li Y, Han S, Ma J. Adsorptive removal of antibiotics from aqueous solution using carbon materials. *Chemosphere*, **2016**,**153**:365-385
- [4]Li Y H, Lai Z, Huang Z J, Wang H Y, Zhao C X, Ruan G H, Du F Y. Fabrication of BiOBr/MoS₂/graphene oxide composites for efficient adsorption and photocatalytic removal of tetracycline antibiotics. *Appl. Surf. Sci.*, **2021**,**550**:149342
- [5]Du F Y, Sun L L, Tan W, Wei Z Y, Nie H G, Huang Z J, Ruan G H, Li J P. Magnetic stir cake sorptive extraction of trace tetracycline antibiotics in food samples: preparation of metal-organic framework-embedded polyHIPE monolithic composites, validation and application. *Anal. Bioanal. Chem.*, **2019**,**411**:2239-2248
- [6]Tian C G, Zhang Q, Wu A P, Jiang M J, Liang Z L, Jiang B J, Fu H G. Cost-effective large-scale synthesis of ZnO photocatalyst with excellent performance for dye photodegradation. *Chem. Commun.*, **2012**,**48**:2858-2860
- [7]Goktas S, Goktas A. A comparative study on recent progress in efficient ZnO based nanocomposite and heterojunction photocatalysts: A review. *J. Alloy. Compd.*, **2021**,**863**:158734
- [8]Weldegebriael G K. Synthesis method, antibacterial and photocatalytic activity of ZnO nanoparticles for azo dyes in wastewater treatment: A review. *Inorg. Chem. Commun.*, **2020**,**120**:108140
- [9]Movahedi T, Norouzebeigi R. Synthesis of flower-like micro/nano ZnO superhydrophobic surfaces: Additive effect optimization via designed experiments. *J. Alloy. Compd.*, **2019**,**795**:483-492
- [10]Wang M, Guo Y Y, Zhu Z Q, Liu Q, Sun T M, Cui H H, Tang Y F. Diethanolamine-assisted and morphology controllable synthesis of ZnO with enhanced photocatalytic activities. *Mater. Lett.*, **2021**,**299**:130114
- [11]伍水生, 易兵, 王染, 兰东辉, 谭年元. ZnO 修饰提升花状 BiOBr 的可见光催化降解罗丹明 B 性能. *无机化学学报*, **2022**,**38**(2):211-219
WU S S, YI B, WANG R, LAN D H, TAN N Y. Enhancing photocatalytic performance of flower-like BiOBr for degradation of rhodamine B by ZnO modification. *Chinese J. Inorg. Chem.*, **2022**,**38**(2):211-219
- [12]姚玉峰, 袁嘉怡, 沈明, 杜彬, 邢蓉. 两亲型杯芳烃诱导 ZnO 微纳结构的合成及光催化性能. *无机化学学报*, **2022**,**38**(2):261-273
YAO Y F, YUAN J Y, SHEN M, DU B, XING R. Synthesis and photocatalytic performance of ZnO micro/nano materials induced by amphiphilic calixarene. *Chinese J. Inorg. Chem.*, **2022**, **38**(2):261-273
- [13]钟伟, 夏颖帆, 翟杭玲, 高越, 李世慧, 吕春欣. 共沉淀法制备稀土 Ce 掺杂的纳米 ZnO 机器光催化降解染料的性能. *无机化学学报*, **2020**,**36**(1):40-52
ZHONG W, XIA Y F, ZHAI H L, GAO Y, LI S H, LÜ C X. Preparation by co-precipitation method and photocatalytic performance on the degradation of dyes of Ce³⁺-doped nano-ZnO. *Chinese J. Inorg. Chem.*, **2020**,**36**(1):40-52
- [14]Kataria N, Garg V K. Removal of Congo red and brilliant green dyes from aqueous solution using flower shaped ZnO nanoparticles. *J. Environ. Chem.*, **2017**,**5**:5420-5428
- [15]Chauhan A K, Kataria N, Garg V. Green fabrication of ZnO nanoparticles using *Eucalyptus spp.* leaves extract and their application in wastewater remediation. *Chemosphere*, **2020**,**247**:125803
- [16]Guo Y Y, Liu N, Sun T M, Cui H H, Wang J, Wang M, Wang M M, Tang Y F. Rational structural design of ZnOHF nanotube-assembled microsphere adsorbents for high efficient Pb²⁺ removal. *CrystEngComm*, **2020**,**22**:7543-7548
- [17]Guo Y Y, Mo Y X, Cui H H, Wang M, Tang Y F, Sun T M. Green and facile synthesis of hierarchical ZnOHF microspheres for rapid and selective adsorption of cationic dyes. *J. Mol. Liq.*, **2021**, **329**:115529
- [18]Yu X Y, Luo T, Jia Y, Xu R X, Gao C, Zhang Y X, Liu J H, Huang X J. Three-dimensional hierarchical flower-like Mg-Al-layered double hydroxides: highly efficient adsorbents for As(V) and Cr(VI) removal. *Nanoscale*, **2012**,**4**:3466-3474
- [19]Zhang G L, Cao D J, Wang X S, Guo S Y, Yang Z Z, Cui P, Wang Q, Dou Y, Cheng S, Shen H. α -Calcium sulfate hemihydrate with a 3D hierarchical straw-sheaf morphology for use as a remove Pb²⁺ adsorbent. *Chemosphere*, **2022**,**287**:132025
- [20]Gao M, Wang W M, Cao M B, Yang H B, Li Y S. Constructing hydrangea-like hierarchical zinc-zirconium oxide microspheres for

- accelerating fluoride elimination. *J. Mol. Liq.*, 2020,317:111133
- [21]El-Nahas S, Abd El-sadek M S, Salman H M, Elkady M M. Controlled morphological and physical properties of ZnO nanostructures synthesized by domestic microwave route. *Mater. Chem. Phys.*, **2021**, **258**:123885
- [22]Cho S H, Jung S H, Lee K H. Morphology-controlled growth of ZnO nanostructures using microwave irradiation: From basic to complex structures. *J. Phys. Chem. C*, **2008**,**112**:12769-12776
- [23]Bao Y, Wang C, Ma J Z. Morphology control of ZnO microstructures by varying hexamethylenetetramine and trisodium citrate concentration and their photocatalytic activity. *Mater. Des.*, **2016**,**101**:7-15
- [24]Lv S, Wang C G, Xing S X. Hexamethylenetetramine-induced synthesis of hierarchical NiO nanostructures on nickel foam and their electrochemical properties. *J. Alloy. Compd.*, **2014**,**603**:90-196
- [25]Gao X D, Li X M, Yu W D. Synthesis and characterization of flower-like ZnO nanostructures via an ethylenediamine-mediated solution route. *J. Solid State Chem.*, **2005**,**178**:1139-1144
- [26]Li C, Lin Y, Li F, Zhu L H, Sun D M, Shen L, Chen Y, Ruan S P. Hexagonal ZnO nanorings: Synthesis, formation mechanism and trimethylamine sensing properties. *RSC Adv.*, **2015**,**5**:80561-80567
- [27]Huang Z B, Zhang Y Q, Tang F Q. Solution-phase synthesis of single-crystalline magnetic nanowires with high aspect ratio and uniformity. *Chem. Commun.*, **2005**,**3**:342-344
- [28]Zhang X, Ai Z H, Jia F L, Zhang L Z. Generalized one-pot synthesis, characterization, and photocatalytic activity of hierarchical BiOX (X = Cl, Br, I) nanoplate microspheres. *J. Phys. Chem. C*, **2008**,**112**:747-753
- [29]Zhong L S, Hu J S, Liang H P, Cao A M, Song W G, Wan L G. Self-assembled 3D flowerlike iron oxide nanostructures and their application in water treatment. *Adv. Mater.*, **2006**,**18**:2426-2431
- [30]Wang M, Yang X, Tian S Q, Guo Y Y, Sun T M, Wang M M, Tang Y F. Constructing novel hierarchical porous hydrangea-like ZnWO₄ microspheres with enhanced photocatalytic performance. *Mater. Lett.*, **2020**,**264**:127417